# Author's Accepted Manuscript


www.elsevier.com/locate/ijadhadh

## Accurate and continuous adhesive fracture energy determination using an instrumented Wedge test

M. Budzik, J. Jumel, K. Imielińska, M.E.R. Shanahan

PII: S0143-7496(09)00015-3
DOI: doi:10.1016/j.ijadhadh.2008.11.003
Reference: JAAD 902

To appear in: *International Journal of Adhesion*

Accepted date: 23 November 2008

Cite this article as: M. Budzik, J. Jumel, K. Imielińska and M.E.R. Shanahan, Accurate and continuous adhesive fracture energy determination using an instrumented Wedge test, *International Journal of Adhesion* (2009), doi:10.1016/j.ijadhadh.2008.11.003

# Accurate and Continuous Adhesive Fracture Energy Determination using an Instrumented Wedge Test

M. Budzik [a,b], J. Jumel [a], K. Imielińska [b], M.E.R.Shanahan [a,*]

[a] Université Bordeaux 1, Laboratoire de Mécanique Physique (LMP)-UMR CNRS 5469, 351 Cours de la Libération, 33405 TALENCE Cedex, FRANCE.

[b] Technical University of Gdansk, Faculty of Mechanical Engineering, Dept. of Material Science and Engineering, Narutowicza 11/12, 80-952 GDANSK, POLAND.

**Abstract**

The wedge test, and the related, double cantilever beam test, are practical methods of assessing structural adhesive fracture energy. In the former, and to a lesser extent the latter, a recognised problem is the difficulty of following the length of the growing crack, required to calculate fracture energy with any accuracy. We present a novel method of measurement of crack length, which has the advantages of being accurate, and allowing continuous assessment of crack length evolution during the failure process. It is based on the attachment of a series of strain gauges to the outer surface of one of the beams constituting the adhesive assembly. Surface strain measurements are interpreted directly using simple beam theory. The method has been validated both with adhesive assemblies under failure conditions, and by tests undertaken on "artificial" joints where "bonding" is effected by clamping adherends together.

**Keywords:** Adhesive bond failure; Crack length; Fracture; Strain gauges; Wedge test

*Corresponding author: Tel: +33 (0)5 40 00 66 11, Fax: +33 (0)5 40 00 69 64, E-mail: m.shanahan@lmp.u-bordeaux1.fr

## 1. Introduction

Of the various adhesion tests available for evaluating the fracture strength of structural adhesive joints, the double cantilever beam (DCB) and its close relative, the (so-called Boeing) wedge test, are amongst the most versatile, and generally yield the most reliable information about fracture energy [e.g. 1-11]. With a judicious choice of test geometry, these systems lead to relatively small adherend strains near the crack front [10, 11]. As a result, local plastic strain, which leads to supplementary energy dissipation, is relatively limited. The main difference between the DCB and the wedge test is that in the former, fracture occurs at imposed *rate of* separation and in the latter, at imposed separation. (The DCB also tends to be used with thicker adherends.)Two adherends are bonded along (most of) their length and with the DCB, a force is applied to each (for example in a tensile testing machine), at the open end and perpendicular to the joint, in order to force debonding [2]. The separation rate of the two points of application of the force is maintained constant. If the length of the opening crack (either within the adhesive or at the interface adherend/adhesive, depending on type of failure) is represented by $a$, it may be shown that the energy release rate, equivalent to fracture energy, $G_c$, follows a scaling rule of the form $G_c \sim a^2$. Beam analysis based on the opening displacement and the force applied allows $a$, and therefore $G_c$, to be evaluated.

However, since the bending moment leading to failure increases linearly with $a$, at constant applied force, crack growth may accelerate and become unstable in certain cases. This problem has been countered by the development of the more refined, *tapered* double cantilever beam test (TDCB), in which stability is restored by using profiled adherends with thickness increasing away from the region of force application [e.g. 4, 12]. (Also, in principle, crack length need not be measured directly.) Notwithstanding, it is not always convenient, or even possible, to use profiled adherends (for instance, when testing the adhesion properties of automotive body assembly materials) and so an alternative set-up is the so-called wedge test, which uses the same geometry, generally of thin plates bonded together, but the opening displacement is maintained constant by insertion of the "wedge" [11]. Crack growth is then "driven" by the restitution of stored, elastic, strain energy stored in the bent adherends, mainly from the wedge up to the crack front [13]. A considerable advantage is that the scaling relation becomes $G_c \sim a^{-4}$ leading to stable crack growth at decreasing rate [14, 15]. The disadvantage is that, since the

force exerted on the adherends by the wedge is unknown, direct measurement of the crack length, $a$, is necessary to calculate $G_c$.

Adherend lengths are typically of the order of 10 cm, and wedge thickness of the order of a few millimetres, and as a consequence, the relatively small curvature of the beams means that the evaluation of crack length may be delicate. Various techniques have been used to study crack lengths in adhesion tests. The most basic techniques rely on direct, or microscopic, observations of the position of the crack tip, sometimes with the addition of paint, or other marking fluid, to the joint edges to facilitate observation [11, 15, 16, 17]. Use has been made of optical correlation [15], laser moiré [18] and speckle interferometry [14]. Electrical techniques have also been tried; such as measurement of crack growth through changes in electrical resistance of carbon paint applied to the edges of non-conducting substrates [19], or by employing piezoelectric techniques [20]. The use of a single strain gauge technique has also been reported [21]. Displacement sensors have been employed for continuously monitoring cracks [11]. Measurement of crack length nevertheless remains a delicate process in many practical cases. In the present contribution, we present a novel method making use of strain gauges attached to the adherends, along the direction of crack propagation. By combining the data from the various strain gauges in their different relative positions with respect to the crack front, an accurate, and potentially continuous assessment of crack length can be obtained. Although the technique of attaching strain gauges to the opposite side of an adherend (from that which is bonded: the "back face") has already been used, previously the joint geometry was generally rather different [22-27].

## 2. Experimental

### *2.1. Materials*

Wedge adhesive test assemblies were constructed from aluminium plates, bonded together using an epoxy adhesive. The system chosen was "asymmetric", in that the two adherends to be bonded were of different thickness. Aluminium plates of alloy 2024, of Young's modulus, $E$, and Poisson's ratio, $\nu$, respectively of *ca*. 70 GPa and 0.33, were obtained from sheets of thickness 5 mm and 1.6 mm, the latter being clad. These represented respectively the "rigid", or thick, and the "flexible", or thin, adherends. Relative flexural rigidity is governed by the ratio of the cubes of thickness (for the same

Young's modulus), thus giving a figure of *ca*. 30. The terms "rigid" and "flexible" are therefore reasonable.

Adherend lengths were 150 mm ("rigid") and 110 mm ("flexible"), and their relative positions, after bonding in a jig, were as indicated in Fig. 1, with a joint width, *b*, of 25 mm. The (initially) unbonded zone on the right corresponded to that of three of the strain gauges, for reasons described below, and also to facilitate insertion of the wedge. The adhesive used was a commercial epoxy resin consisting of bisphenol A of average molecular weight < 700 cured with N (3 dimethylaminopropyl) – 1, 3 propylenediamine. Crosslinking was effected at ambient temperature (*ca.* 20°C) for 24 hours under 2 bars pressure and at *ca*. 55 % RH. Bondline thickness was maintained at *ca*.0.35 mm (measured by optical microscopy), by inserting PTFE spacers at the two point extremities before crosslinking. The constancy was checked by optical microscopy.

The main aim of this contribution is to report a new development for measuring strain, and thus obtain crack length in the wedge test, and to corroborate results we have employed two different surface preparations of the aluminium prior to bonding. Both aluminium surfaces to be bonded in a given joint were prepared in an identical manner, either by simple abrasion or by an electrochemical treatment. For both types of preparation, the initial procedure was surface degreasing with detergent solution, drying in hot air, rinsing in acetone, followed by light abrasion/polishing with 1200 grade emery paper. In the case of the simple abrasive treatment, this was followed up by abrasion with 400 grade emery paper and distilled water rinsing, drying in hot air and rinsing in acetone.

In the case of the electrochemical treatment, after the light 1200 grade emery abrasion, further detergent cleaning, hot air drying and acetone rinsing preceded immersion in an electrochemical bath. Phosphoric acid anodisation (PAA) was adopted, using a solution of 10% (by weight) of phosphoric acid ($H_3PO_4$) in deionised water, under a 10 volt direct current potential for 20 minutes at *ca*.20°C [28]. The aluminium served as the cathode and a titanium anode was used. After treatment, surfaces were rinsed in distilled water, hot air dried and finally acetone rinsed.

Examples of the final surface topography of the simply abraded and electrochemically treated surfaces obtained by Atomic Force Microscopy (AFM) are shown in Fig. 2. (The apparatus used was a Digital Instruments (Veeco Metrology

Group) Nanoscope®). It is clear that the anodisation gives a much rougher, or more "peaky" surface topography.

In some experiments, detailed below, surface preparation was of no importance, since no adhesive bonding was performed: a controllable, "artificial" bonded joint was employed instead.

*2.2. "Artificial" wedge test*

This technique was employed in order to estimate the accuracy of the strain gauge technique developed here, without using an actual *adhesive* joint. The same aluminium adherends as described above, of thicknesses 5 and 1.6 mm, were employed, but instead of bonding them together with an adhesive, a simple screw-based, collar-like clamping system was devised, which could be slid over the "joint" section, i.e. both adherends were placed together, as though bonded, and secured at a desired value of $x$, equivalent to "crack-length", $a$ (see Fig. 3). The joint would be effectively unbonded for $x$ less than the value chosen and bonded for $x$ greater, $x$ being directly measurable. Strain gauges were bonded in place along the central line of the thin adherend, at values of $x$ of 16, 26, 36 and 46 mm. Strain measurements were taken with two wedge thicknesses, $\Delta$, of 4.6 and 9.7 mm, and three "beam lengths", $a$: 64, 75 and 90 mm for $\Delta = 4.6$ mm, and 75, 90 and 102 mm for $\Delta = 9.7$ mm. This technique permitted both the fabrication of "artificial" wedge-type joints, described here, by the clamping of unbonded aluminium plates at a desired value of $x$, before wedge insertion, and also the "reconstitution" of bonded wedge samples, either partially or totally separated during prior tests, both to corroborate crack-length evaluation and check that plastic adherend deformation had not occurred during a test. However, due to the imposed, straight "crack-front" parallel to the $y$ axis in this technique, any effects due to anticlastic bending, or other phenomena leading to non-rectilinear fracture fronts are necessarily neglected [14]. Similarly, any possible influence of a deformable elastic foundation ahead of the crack front, or root rotation, is neglected [13, 15, 29, 30].

*2.3. Asymmetric wedge test (AWT)*

The principal experimental technique used here to estimate crack length, $a$, depends on the use of strain gauges bonded to a flexed "beam" corresponding to the

separated section of the adhesive joint. It is clear that for reasons of economy in gauges, it is better to adopt the asymmetric form of the wedge test (AWT), with one "rigid" adherend, obviating the application of gauges on both joint arms. In addition, with a supposedly symmetrical system, any slight discrepancies in bending behaviour of the two members could render it difficult to interpret strain gauge measurements.

Referring to Fig. 1, five longitudinal strain gauges (Vishay Micro-Measurements, reference EA - 13 - 060LZ - 120/E, of nominal resistence120 Ω) were fixed to the upper, exposed, side of the "flexible" adherend, along the centre line and at distances $x_i$ from the origin, defined as the position of contact of the two joint arms with the inserted wedge. The values of $x_1$ to $x_5$ were respectively 35, 45, 55, 75 and 85 mm. Thus, initially, two strain gauges are within the limits of the bonded region, and three without. A "wedge" of aluminium of thickness, Δ, either of 4.6 or 9.7 mm, was inserted manually to the desired position, corresponding to the origin of $x$, and the adherend separation left to continue at its self-determined rate, whilst strain gauge recordings were made continuously using a Wheatstone bridge arrangement (Vishay Micromesures 2100 System Multi Channel Signal Conditioner/Amplifier with five modules of Model 2120 B Strain Gauge Conditioner/Amplifier, and one module of Model 2110 B Power Supply). Values of strain thus evaluated correspond to (negative) surface strains at $h/2$ from the adherend neutral surface, and at the various values of $x_i$ given above.

Preliminary tests reported here, for each of the two surface treatments, were effected at 20 ± 2°C, and at an ambient humidity of *ca.* 55% RH.

## 3. Results and discussion

### *3.1. Interpretation of strain gauge measurements*

The values of strain on the outer surface of the "flexible" adherend at various values of $x$, the distance between strain gauge (centre) and inserted wedge, are the data we have available from the experimental system described above. Interpretation is made as follows. We assume in the following that the wedge test may be satisfactorily analysed as a two-dimensional problem. Adopting the Cartesian coordinate system shown on the wedge test set-up in Fig. 3, simple beam theory may be used to evaluate the deflection (of

the neutral surface) of the "flexible" adherend, *z(x)*, as a function of the distance, *x*, from the wedge at $x = 0$:

:

$$z(x) = \frac{F}{EI}\left(\frac{1}{6}x^3 - \frac{1}{2}a^2 x + \frac{1}{3}a^3\right) \quad (1),$$

where *a* is separation, or crack, length, *F* is the upward force acting on the beam at the wedge contact, *E* is Young's modulus and $I = bh^3/12$, *b* and *h* representing (thin) adherend width and thickness. In Eq. (1), no allowance has been made for shear due to *F*, in the *z* direction within the adherend [21], but given the inherent flexibility due to a low ratio of *h*/*a*, this is considered to be reasonably negligible. Using standard boundary conditions of $z(a) = dz/dx(a) = 0$ (neglecting any effects of elastic foundation [13, 15, 29, 30]), and with $z(0) = \Delta$, it may be readily found that force, *F*, and wedge thickness, Δ, are simply related by $z(0) = \Delta = Fa^3/(3EI)$, leading to:

$$z(x) = \frac{\Delta}{2}\left(\left(\frac{x}{a}\right)^3 - 3\left(\frac{x}{a}\right) + 2\right) \quad (2).$$

The second differential of *z(x)*, $z_{xx}(x)$, obtained from Eq. (2), is very nearly equal to local adherend curvature at *x*, that is, $R^{-1}(x)$, provided $z_x(x) << 1$. Assuming the adherend to be isotropic and homogeneous, and of constant thickness, *h*, its strain on the *outer* (i.e.unbonded) surface, $\varepsilon_s = \varepsilon(h/2)$ (which is generally negative), is also directly related to local curvature:

$$\left|\varepsilon_s(x)\right| = \left|\varepsilon(x, h/2)\right| = \frac{1}{2}\frac{h}{R(x)} = \frac{1}{2}hz_{xx}(x) \quad (3).$$

Thus we obtain from Eqs (2) and (3):

$$\left|\varepsilon_s(x)\right| = \frac{3\Delta hx}{2a^3} \quad (4),$$

and we therefore have a linear relationship between $\left|\varepsilon_s(x)\right|$ and *x*, for a given crack length, *a*. In principle, it possible to ascertain *a*, and its evolution with time, *t*, *a*(*t*), from

measurements of $|\varepsilon_s(x)|$, with a knowledge of Δ, $h$ and a single value of $x$ from the geometry of the joint, with the proviso that the value of $x$ in question is in the unbonded section of the adherend, and greater than 0. (Young's modulus is not required, as long as it is constant.) However, it is clearly wiser to estimate crack length from several measurements of $|\varepsilon_s(x)|$, at different values of $x$, both in order to check the reproducibility of the procedure and to consider potential errors. With several strain gauges in place, at positions defined by the $x_i$, as described above, we may do this using a statistical treatment.

Since Eq. (4) indicates zero surface strain at $x = 0$, irrespective of time, as may be expected from the fact that there is no bending moment at the origin, it seems natural to apply a one parameter regression analysis to data pertaining to Eq. (4). In other words, we wish to optimize the parameter $\alpha$ in $|\varepsilon_s(x,t)|=\alpha(t)x$, where $\alpha(t) = 3\Delta h/(2a^3(t))$, and then evaluate $a(t)$. This is a straightforward, elementary problem of statistical methods, of which the rudiments are presented in the Appendix. Having established the value $\alpha$ for a given system and at a given time, $t$, (N.B. continuous recording is possible with this technique), we rearrange Eq. (4) and substitute $\alpha(t)$ for $|\varepsilon_s(t)|/x$ to estimate *a(t)*:

$$a(t)=\sqrt[3]{\frac{3\Delta h}{2\alpha(t)}} \qquad (5).$$

Errors on both $\alpha$ and on $a$ have been calculated using Eqs. (A1.3) and (A1.4), given in the Appendix 1.

*3.2. Application to "artificial" wedge test*

The "artificial" wedge test allows us to estimate the value of $a$, given by Eq. (5). Accepted values of "crack length", $a$, correspond to direct measurements from the position of the extremity of the clamping device with respect to the wedge end. An accuracy of $\Delta a = \pm 0.5$ mm would seem reasonable as a practical upper limit to the accuracy, given the possibility of skew loading or other slight misalignment. Fig. 4 shows surface strain, $\varepsilon_s$, *vs* position of strain gauge, $x$, for both 4.6 mm and 9.7 mm wedges, respectively with "crack lengths" of 64, 75 and 90 mm, and of 75, 90 and 102 mm. The

linear relationship expected from Eq. (4) is well obeyed by the experimental measurements, and corresponding regression lines are shown. Coefficients of determination, $R^2$, are also given, and as can be seen, are virtually equal to 1. This confirms that the elementary assumptions made in applying simple beam theory (*cf*. Eqs. (1) and (2)) are a most satisfactory approximation. By applying Eqs.(5) and (A1.4), it was possible to calculate $(a \pm \Delta a)$ and compare the values obtained with those obtained by direct measurement. A summary of these values is presented in Table 1. As can be seen, the agreement between the two sets of data is extremely good, confirming the validity and the precision of the strain gauge method developed. No effects due to anticlastic bending perturbing the crack-front from its rectilinear form are allowed for with this "artificial" crack set-up, but since these are generally relatively small, use of the method is an acceptable technique for validation. These experiments were quite repeatable, confirming that the elastic limit of the aluminium beam had not been exceeded (no observable plastic hysteresis). This may be confirmed from Eq. (4). The greatest value of $|\varepsilon_s(x)|$ is found at the "crack" front, i.e. $|\varepsilon_s(x)|_{\max} = |\varepsilon_s(a)| = 3\Delta h/(2a^2)$. In the most extreme cases for the two wedge thicknesses, we have $\Delta$ = 4.6 mm and $a$ = 64 mm, $h$ being 1.6 mm, and $\Delta$ = 9.7 mm and $a$ = 75 mm, leading respectively to (absolute) surface strains of 0.27% and 0.41%. The yield strain of the aluminium used is of the order of 0.45- 0.5%.

*3.3. Application to adhesive joints*

The evaluation of crack propagation kinetics can be virtually continuous with this strain gauge technique, leading to detailed crack monitoring. Fig. 5 and Fig. 6 represent crack length, $a$, *vs* time, $t$, respectively for the abraded and the PAA treated wedge tests, using a wedge of thickness 9.7 mm. As in the case of the "artificial" wedge test, crack length, $a$, was evaluated using Eq. (5). In these preliminary tests, it was not found practical to initiate crack propagation in wedge test mode from the very end of the bonded region: the opening had to be gently "coaxed" before the wedge was put in place for the static test. This explains the rather large initial crack length reported for the PAA treated joint shown. In the examples shown, the former, for the abraded surface, corresponds to results obtained with three strain gauges, *viz*. at 35, 45 and 55 mm from the wedge. Those at 75 and 85 mm were within the bonded section for the time range studied. All five strain gauges could be employed for the example with PAA treatment. "Noise" on the measurement of $a$ is typically less than $10^{-4}$ m, and at worst less than 2 x

$10^{-4}$ m. This noise has been removed in Figs 5 and 6, for aesthetic reasons, since it only essentially thickens the graphic line. Error bars, shown for various values of time, $t$, were calculated using Eq.(A.4) and those associated. Estimated values of adherend thickness, $\Delta h$, and wedge thickness, $\Delta\Delta$, as evaluated from micrometer measurements, were 0.02 mm. $\Delta E$ was estimated at 0.8 GPa.

As can be seen, estimated errors, $\Delta a$, are similar for the two treatments and reasonably independent of crack length, being of the order of $\pm 0.5$ mm. In fact, this value of $\Delta a$ is similar in magnitude to variations in $a(y)$ expected from anticlastic effects [14], and therefore at the limit of useful precision, given the (still) limited understanding of the crack front curvature. The general features of wedge tests results are present in both cases, *viz*. continuously increasing crack length, $a(t)$, with time, $t$, and concomitant decrease of $da(t)/dt$, as strain energy release rate diminishes. This is a typical trait of adhesive fracture, as exemplified with elastomers many years ago [e.g. 31, 32]. Despite these overall trends, there are "second order" changes in gradient, with slight ups and downs, which are presumably related to a degree of inhomogeneity of the adhesive joint. Such effects are rarely reported in the literature, possibly quite simply because most techniques for measuring crack length cannot be employed in continuous mode, in contrast to the present method. Direct observation of the bondline showed on occasion, although a systematic study was not made, that a type of cavitation sometimes occurred. The basic crack progressed somewhat, but leaving an adhesive bridge between the substrates behind, rather like crazing in a bulk polymer. This would, of course modify the stress distribution, particularly in the proximity of the crack front, but less so removed from this region due to St Venant's principle, and could possibly explain these second order undulations in the plots of *a vs t*, as calculated from strain gauge measurements and using the interpretation described above. However, further work is required to clarify this phenomenon more systematically.

It may be noted that, at the very beginning of the test on the abraded aluminium treated joint shown, the maximum surface strain, $\left|\varepsilon_s(x)\right|_{\max} = \left|\varepsilon_s(a)\right|$, is *ca*. 0.5%, which is close to, if not slightly exceeding, the yield strain of the adherend. Nevertheless, no permanent deformation of the adherend was observed. (The "reconstituted" joint led to reproducible surface strain values, and did not reveal any permanent set.) Of course, as the crack progresses, this value, corresponding to the value of surface strain at the *moving* crack front, quite rapidly decreases. Notwithstanding, for the PAA treated joint,

$|\varepsilon_s(a)|$ is *ca*. 0.26, which is well below the limit. In a correctly designed test procedure, this potential exceeding of the elastic limit of the adherend should, needless to say, be avoided.

*3.4. Fracture Energy*

Interpretation of Fig. 5 and Fig. 6 has been effected using classic equations for the asymmetric wedge test, adapted for the case of one flexible adherend [e.g. 14]. To summarise the procedure, the elastic, strain energy, *U*, stored in the bent beam, or thin substrate, is given by:

$$U = \int_0^a \frac{M}{2R} dr = \frac{EI}{2} \int_0^a (z_{xx})^2 \, dx = \frac{3EI\Delta^2}{2a^3} \qquad (6),$$

where $M = EI/R = Fx$ is the bending moment (*cf*. Eqs.(1) and (2) and associated description). The strain energy release rate is given by:

$$G + \frac{1}{b}\frac{\partial U}{\partial a} = 0 \qquad (7).$$

Since $G = G_c$ at fracture, $G_c$ being the energy of adhesion, Eqs. (6) and (7) lead to:

$$G_c = \frac{3E\Delta^2 h^3}{8a^4} \qquad (8).$$

Although Eq.(8) implicitly concerns mode I fracture, due to the asymmetry of the present geometry, it may be wondered if the mode II contribution is significant. As shown in Appendix 2, mode II is completely negligible.

Fracture, or adhesion, energy, $G_c$, was evaluated for continuously increasing $a(t)$ using Eq. (8) for the two adhesive systems studied using the data presented in Figs 5 and 6. Corresponding crack growth rates, $da(t)/dt$, were also calculated from tangents to the *a vs t* curves. In Fig.7, we present results of $G_c$ *vs* $da(t)/dt$ for the two systems

corresponding to simple abrasive treatment of substrates and PAA treatment. The smaller error bars were calculated assuming an error *only* on $a$, in other words, by using Eq. (A1.5) with $\Delta E$, $\Delta\Delta$ and $\Delta h$ taken to be zero. This is to show the potential precision on $G_c$ obtainable from crack length measurement with the strain gauge method presented here. In order to be more complete, an example of an error bar obtained from Eq. (A1.5), but with $\Delta E$ taken realistically as 0.8 GPa, and both $\Delta\Delta$ and $\Delta h$ as 0.02 mm, is given for each surface treatment. These larger error bars take into account systematic, as well as random errors. We approximately double the estimated error by allowing also for these systematic errors in $E$, $\Delta$ and $h$.

Various observations may be made. Firstly, overall the fracture energies are relatively low for this type of joint [14]. However, the adhesive used was a general-purpose epoxy, and not a specialised material, so this is perhaps not too surprising. Secondly, clearly the PAA surface treatment gives a considerably higher fracture energy than simple abrasive treatment, for any given crack growth rate. At the lower end of the rate scale studied, fracture energy is *ca.* 80% greater for PAA, at the other extreme, *ca.* 20%. Nevertheless, for both surface treatments, an increase in crack speed reflects an increase in fracture energy, as may be expected from a higher level of energy dissipation. This suggests that the relation between effective energy of adhesion and surface treatment is not simply multiplicative, as often suggested for elastomers [e.g. 31, 32]. Superficially at least, fracture appeared to be interfacial for the abraded aluminium surfaces, but distinctly cohesive within the adhesive for the PAA pre-treatment. Again, this is not surprising as good adhesion to aluminium generally requires adequate surface treatment. However, we shall not dwell on this, as the main object of this contribution is to present a novel, we believe, technique to measure crack lengths. These preliminary results on "real" joints in this context are presented to corroborate findings with the "artificial" wedge tests.



## 4. Conclusions

The wedge test is a useful test for the assessment of structural adhesive fracture energy. However, a recurrent problem is the difficulty often encountered in obtaining good precision in the measurement of crack length, $a$, needed to calculate fracture energy, $G_c$. Given the dependence of $G_c$ on $a^{-4}$, potential, relative errors in $a$ become fourfold in $G_c$ (assuming standard propagation of errors theory). We have developed a method for assessment of crack length based on attaching strain gauges to the outer surface of one of

the adherends constituting the joint to be tested in fracture. By applying simple beam theory to a knowledge of the surface strains monitored at various places on the adherend, or "beam", an accurate assessment of crack length can be obtained. The method has been investigated using "artificial" joints, in which aluminium plates were clamped together, thus enabling easy, direct determination of "crack" length, for comparison. Results indicate that the approximations of simple beam theory are quite adequate for obtaining good estimations of crack length. These findings were corroborated by application to the fracture results of "real", adhesive joints. Apart from the advantages of accuracy and simplicity, the method presents other advantages. Continuous measurement of crack length, $a$, becomes possible, potentially useful for studying the "fine structure" of a $G_c$ *vs* $da(t)/dt$ curve. By "reconstituting" adhesive joints, and/or reconsidering surface strain after fracture, it should be possible to detect any plastic strain in the adherends, due to excessive curvature.

**References**

[1] E.J. Ripling, S. Mostovoy, R.L. Patrick, Mater Res Standards (ASTM Bulletin) 1964; 4: 129–134.

[2] S. Mostovoy, E.J.Ripling, J Appl Polym Sci 1966; 10: 1351-1371.

[3] S. M. Wiederhorn, A.M. Shorb, R.L.Moses, J Appl Mech 1968; 39: 1569-1572.

[4] S. Mostovoy, E.J.Ripling, J Appl Polym Sci 1969; 13: 1083-1111.

[5] M.F. Kanninen, Int J Fracture 1974; 10: 415-430.

[6] H. Kollek, Int J Adhesion Adhesives 1985; 5: 75 – 80.

[7] J.M.Whitney, Comp Sci Tech 1985; 23: 201-219.

[8] B. Blackman, J.P. Dear, A.J. Kinloch, S. Osiyemi, J Mater Sci Lett 1991; 10: 253-256.

[9] J.K. Jethwa, A.J. Kinloch, J Adhesion 1997; 61:71-95.

[10] M. Meiller, A.A. Roche, H. Sautereau, J Adhesion Sci Tech 1999 ; 13: 773-788.

[11] J.Y. Sener, T. Ferracin, L. Caussin, F. Delannay, Int J Adhesion Adhesives 2002; 22: 129 – 137.

[12] B. R. K. Blackman, H. Hadavinia, A. J. Kinloch, M. Paraschi, J. G. Williams, Eng Fract Mech 2003; 70: 233-248.

[13] M.F. Kanninen, Int J Fracture 1973; 9: 83-92.

[14] S. Popineau, B. Gautier, P. Slangen, M.E.R. Shanahan, J Adhesion 2004; 80:1173-1194.

[15] J.P. Sargent, Int J Adhesion Adhesives 2005; 25: 247 – 256.

[16] H. Aglan, Z. Abdo, J Adhesion Sci Tech 1996; 10: 183-198.

[17] B. R. K. Blackman, A. J. Kinloch, M. Paraschi, W. S. Teo, Int J Adhesion Adhesives 2003; 23: 293 – 305.

[18] R.Davidson, Proceedings of the SPIE - The International Society for Optical Engineering 1988; 814: 479-89.

[19] H. Nayeb-Hashemi, D. Swet, A. Vaziri**,** Measurement 2004; 36: 121-129.

[20] H.Y. Hwang, B.J. Kim, W.S. Chin, H.S. Kim, D.G. Lee, J Adhesion Sci Tech 2005; 19: 1081-111.

[21] P.B. Crosley, E.J. Ripling, J Testing Evaluation 1991;19: 24-28.

[22] Z.Zhang, J.K.Shang, J Adhesion 1995; 49: 23-36.

[23] A.J. Curley, H. Hadavinia, A.J. Kinloch, A.C. Taylor, Int J Fract 2000; 103: 41-69.

[24] A. D. Crocombe, C.Y. Ong, M.M. Abdel-Wahab, J Adhesion 2002; 78: 745-776.

[25] H. Hadavinia, A.J. Kinloch, M.S.G. Little, A.C. Taylor, Int J Adhesion Adhesives 2003; 23: 449-461.

[26] J.F. Destrebecq, M.Grediac, V. Sierra-Ruiz, Compo Sci Tech, 2007; 67: 707-719.

[27] A. Gacoin, A. Objois, J. Assih, Y. Delmas, J Adhesion 2008; 84: 37-59.

[28] R.P. Digby, D.E. Packham, Int J Adhesion Adhesives 1995; 15: 61-71.

[29] J.G. Williams, J Adhesion 1993; 41: 225-239.

[30] B. Cotterell, K. Hbaieb, J.G. Williams, H. Hadavinia, V. Tropsa**,** Mech Mater 2006; 38: 571-584

[31] A.N. Gent, R.P.Petrich, Proc Roy Soc (London) 1969; A310: 433-448.

[32] D. Maugis, M. Barquins, J Phys D 1978; 11: 1989-2033.

**Appendix 1: Estimation of errors**

To obtain the best estimate of the parameter $\alpha$ from experimental data, assuming a functional relation, $\varepsilon = \alpha x$, between the independent variable, $x$, and the dependent variable, $\varepsilon$, we have used the usual regression, or least squares, principle. (The more cumbersome notation of $|\varepsilon_s(x)|$ in the main text has been simplified to $\varepsilon$, or $\varepsilon_i$, the suffix representing the term in the following summations from 1 to $n$.) ) Minimisation of the summation, over the $n$ available values, of $\sum_{i=1}^{n}(\varepsilon_i - \varepsilon)^2 = \sum_{i=1}^{n}(\varepsilon_i - \alpha x_i)^2$ with respect to $\alpha$ is the required criterion, where $\varepsilon_i$ is the *experimental* value and $\varepsilon$ represents the *expected* value, from $\varepsilon = \alpha x$, for the $x_i$ in question. The summation is differentiated with respect to $\alpha$, and the result set equal to zero, leading, after rearrangement, to:

$$\alpha = \frac{\sum_{i=1}^{n} x_i \varepsilon_i}{\sum_{i=1}^{n} x_i^2} \qquad \text{(A1.1).}$$

The best estimate of the standard deviation of $\varepsilon$ is given by the well-known expression:

$$s_n(\varepsilon) = \frac{\sum_{i=1}^{n}(\varepsilon_i - \alpha x_i)^2}{(n-1)^{1/2}} \qquad \text{(A1.2),}$$

and since the various values of $\varepsilon_i$ are expected to have (more or less) the same confidence, their weightings are taken as equal in the assessment of $\alpha$, thus leading to an expression for the standard error, $\Delta\alpha$, on $\alpha$ (equal to the best estimate of the standard deviation, as one assessment only is involved):

$$\Delta\alpha = \frac{s_n(\varepsilon)}{\left(\sum_{i=1}^{n} x_i^2\right)^{1/2}} = \frac{\left\{\sum_{i=1}^{n}\varepsilon_i^2 - \left(\sum_{i=1}^{n} x_i \varepsilon_i\right)^2 \Big/ \sum_{i=1}^{n} x_i^2\right\}^{1/2}}{(n-1)^{1/2}\left(\sum_{i=1}^{n} x_i^2\right)^{1/2}} \qquad \text{(A1.3).}$$

Expressions (A1.1) and (A1.3) then allow estimates of $(\alpha \pm \Delta\alpha)$ to be incorporated in the overall expressions both for crack length, $a(t)$ (i.e. Eq. (5)), and its estimated potential error, $\Delta a(t)$, calculated from the formula for propagation of errors, allowing for uncertainties in the accepted values of adherend, $\Delta h$, and wedge thicknesses, $\Delta\Delta$:

$$\Delta a = \frac{a}{3}\left\{\left(\frac{\Delta h}{h}\right)^2 + \left(\frac{\Delta\Delta}{\Delta}\right)^2 + \left(\frac{\Delta\alpha}{\alpha}\right)^2\right\}^{1/2} \qquad \text{(A1.4).}$$

Eq. (A1.4) was used to calculate the error bars shown in Figs. 5 and 6.

The main, small, error bars on $G_c$, in Fig. 7, were calculated assuming only intrinsic error on $a$ (Eq. (A1.4)) It is, however, also of interest to calculate potential errors on the evaluation of fracture, or adhesion, energies, taking all (reasonable) potential errors into account.. In the basic expression for fracture energy, $G_c$, given by Eq.(8), there are four parameters presenting potential errors, *viz*. $E$, $\Delta$, $h$ and $a(t)$. Having evaluated $\Delta a$ from Eq.(A1.4), and with estimates of the other three, we may employ standard error propagation methods to arrive at an estimate of the precision of the calculated fracture energy, $\Delta G_c$:

$$\Delta G_c = G_c\left\{\left(\frac{\Delta E}{E}\right)^2 + 4\left(\frac{\Delta\Delta}{\Delta}\right)^2 + 9\left(\frac{\Delta h}{h}\right)^2 + 16\left(\frac{\Delta a}{a}\right)^2\right\}^{1/2} \qquad \text{(A1.5).}$$

The two larger error bars in Fig. 7 correspond to use of Eq. (A1.5).

It is perhaps worth noting that any error on $\Delta$ ought to be systematic, for a given experiment. Given the form of Eq. (8), this implies that a simple translation of $G_c$ *vs* $da(t)/dt$ would result.

**Appendix 2: Mode II contribution to fracture**

Since the asymmetric wedge test studied here may, in principle, invoke a degree of mode II fracture in addition to the principal mode I, we present a simple analysis showing, in the present case at least, that the former contribution is negligible.

Consider initially the geometry shown in Fig. A2.1, which represents two thick substrates bonded such that failure is occurring parallel to the interface, in mode II, due to the application of force, *f*. (The lower adherend is considered fixed.) If the force is stationary, but the crack grows by an increment $\delta a$, the elastic strain energy density in the volume *abh* (where *b* is width) is reduced, since *f* decreases, although the volume involved increases to $(a+\delta a)\,bh$. The net result is a reduction in overall stored energy, and it is this that drives the crack in mode II, requiring energy $G_{IIc}.\,b.\,\delta a$. From an energy balance, it can be readily shown (cf. Eq. (7)) that the mode II fracture energy, $G_{IIc}$, is given by:

$$G_{IIc}=\frac{f^2}{2Ehb^2} \qquad \text{(A2.1).}$$

Now consider the wedge/beam contact zone of Fig.3, magnified in Fig A2.2. Assuming friction to be negligible, the vertical force, *F*, introduced in Eq.(1) is, in fact, the vertical component, $\widetilde{F}\cos\alpha$, of the contact force, $\widetilde{F}$, normal to the beam (although the difference is very small for small $\alpha$). Similarly, there also exists a (small) horizontal component, *f*, given by $\widetilde{F}\sin\alpha$. From $z_x(0)$, evaluated using Eq.(2), and the fact that $\Delta=Fa^3/(3EI)$, we may write force, *f*, as:

$$f=F\left|\frac{dz}{dx}\right|_{x=0}=\frac{9\Delta^2 EI}{2a^4} \qquad \text{(A2.2).}$$

In the above, as before, we neglect any possible effects of root rotation.

Ignoring the bending aspect of the beam caused by $\widetilde{F}\cos\alpha$, we may assimilate the mode II component of fracture in the wedge test with the above and employ Eq. (A2.1) to estimate mode II fracture energy.

Combining Eq (A2.1) and (A2.2), and with the definition of $I$ (= $bh^3/12$), we obtain:

$$G_{IIc}=\frac{9\Delta^4 h^5 E}{128a^8} \qquad \text{(A2.3).}$$

Finally, using the definition of $G_c$ (Eq.(8)), which may be written more precisely as $G_{Ic}$ in the present context, we may estimate the relative importance of mode II fracture compared with mode I, from the ratio:

$$\frac{G_{IIc}}{G_{Ic}}=\frac{3\Delta^2 h^2}{16a^4} \qquad \text{(A2.4).}$$

With the present experiments, the "worst" case corresponds to the following values: $h$ =1.6 mm, $\Delta$ = 9.7 mm and $a$ = 75 mm. These values lead to a ratio of mode II to mode I fracture energies of ca. 1.5 x $10^{-6}$. Clearly, neglect of mode II is this asymmetric test is of no consequence, although it may be with other geometries.

**Table**

| | *Direct measurement* | | *Strain gauge estimate* | |
|---|---|---|---|---|
| ***Wedge thickness, Δ (mm)*** | ***a (mm)*** | ***Δ a (mm)*** | ***a (mm)*** | ***Δ a (mm)*** |
| 4.5 | 64 | 0.5 | 63.8 | 0.4 |
| | 75 | 0.5 | 74.8 | 0.3 |
| | 90 | 0.5 | 89.9 | 0.4 |
| 9.7 | 75 | 0.5 | 74.3 | 0.4 |
| | 90 | 0.5 | 88.9 | 0.4 |
| | 102 | 0.5 | 101.2 | 0.5 |

**Table 1:** Estimates of crack length, $a$, and possible error $\Delta a$, for two values of wedge thickness, $\Delta$, both by direct measurement in the "artificial" wedge test, and by the strain gauge technique.

## Figure Legends

**Fig. 1.** Representation of geometry of asymmetric wedge test sample. (Dimensions in mm.)

**Fig. 2**. Atomic Force Micrographs of (a) simply abraded aluminium, and (b) electrochemically treated surfaces.

**Fig. 3.** Sketch of geometry of asymmetric wedge test with nomenclature used.

**Fig. 4.** Surface strains, $|\varepsilon_s(x)|$, obtained from strain gauge measurements, *vs* positions, $x$, of strain gauges ($x$ = 16, 26, 36 and 46 mm) and corresponding linear regression lines, for wedges of both thicknesses, 4.6 and 9.7 mm . The three lines in each graph correspond to imposed "crack lengths", $a$, given in the left upper corner.

**Fig. 5.** Results of crack length, $a$, *vs* time, $t$, for wedge test with abrasive prepared surfaces.

**Fig. 6.** Results of crack length, $a$, *vs* time, $t$, for wedge test with PAA prepared surfaces.

**Fig. 7.** Fracture, or adhesion, energy, $G_c$, *vs* crack growth rate, $da(t)/dt$ , for wedge tests after abrasive and after PAA surface treatments prior to adhesive bonding with epoxy resin. Smaller error bars are only representative and could be calculated for any value of $da(t)/dt$ . They correspond to the result of errors *only* on $a$. The two larger bars, one on each curve, represent overall errors taking into account systematic effects of $E$, $\Delta$ and $h$.

**Fig.A2.1** Model for mode II fracture.

**Fig A2.2** Close of wedge/beam contact zone.

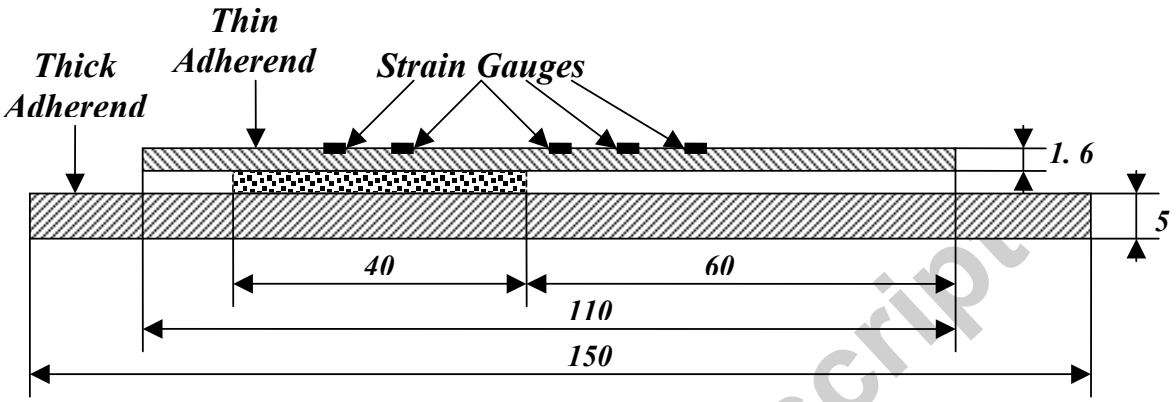


**Fig. 1.** Representation of geometry of asymmetric wedge test sample. (Dimensions in mm.)

(a)

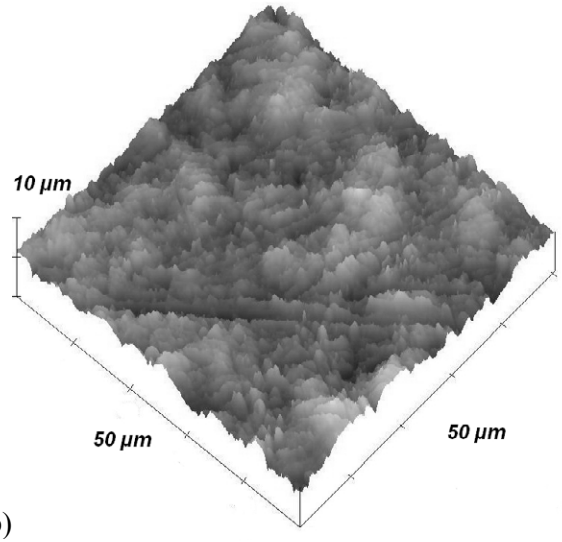


(b)

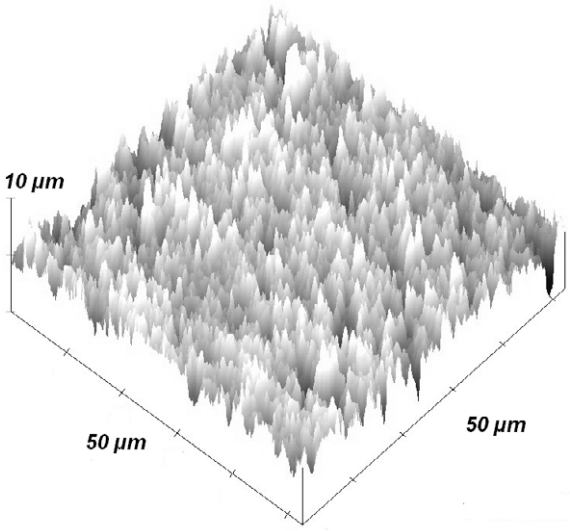


**Fig. 2**. Atomic Force Micrographs of (a) simply abraded aluminium, and (b) electrochemically treated (PAA) surfaces.

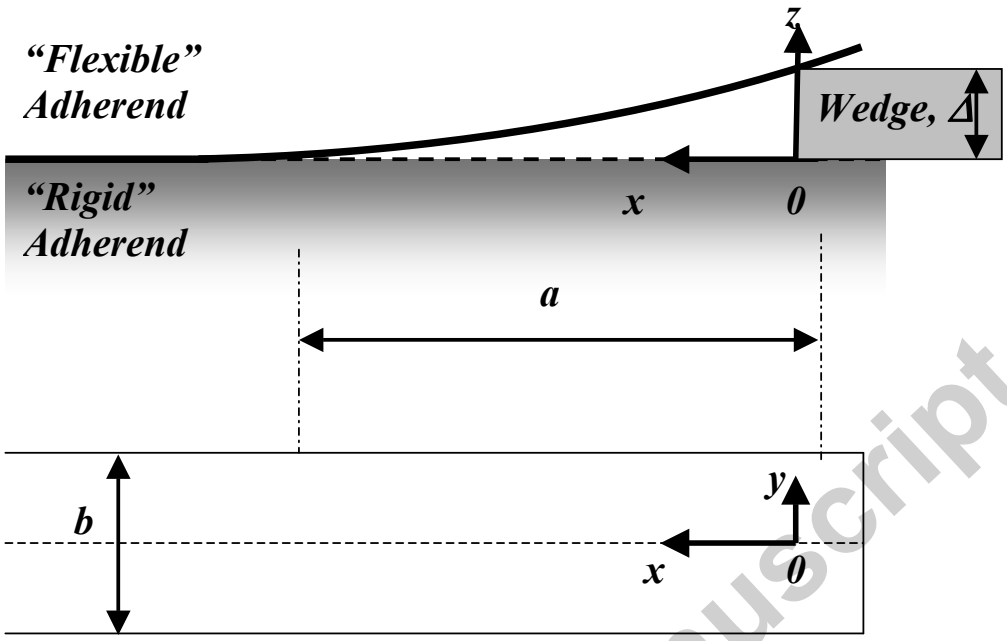


**Fig. 3.** Sketch of geometry of asymmetric wedge test with nomenclature used.

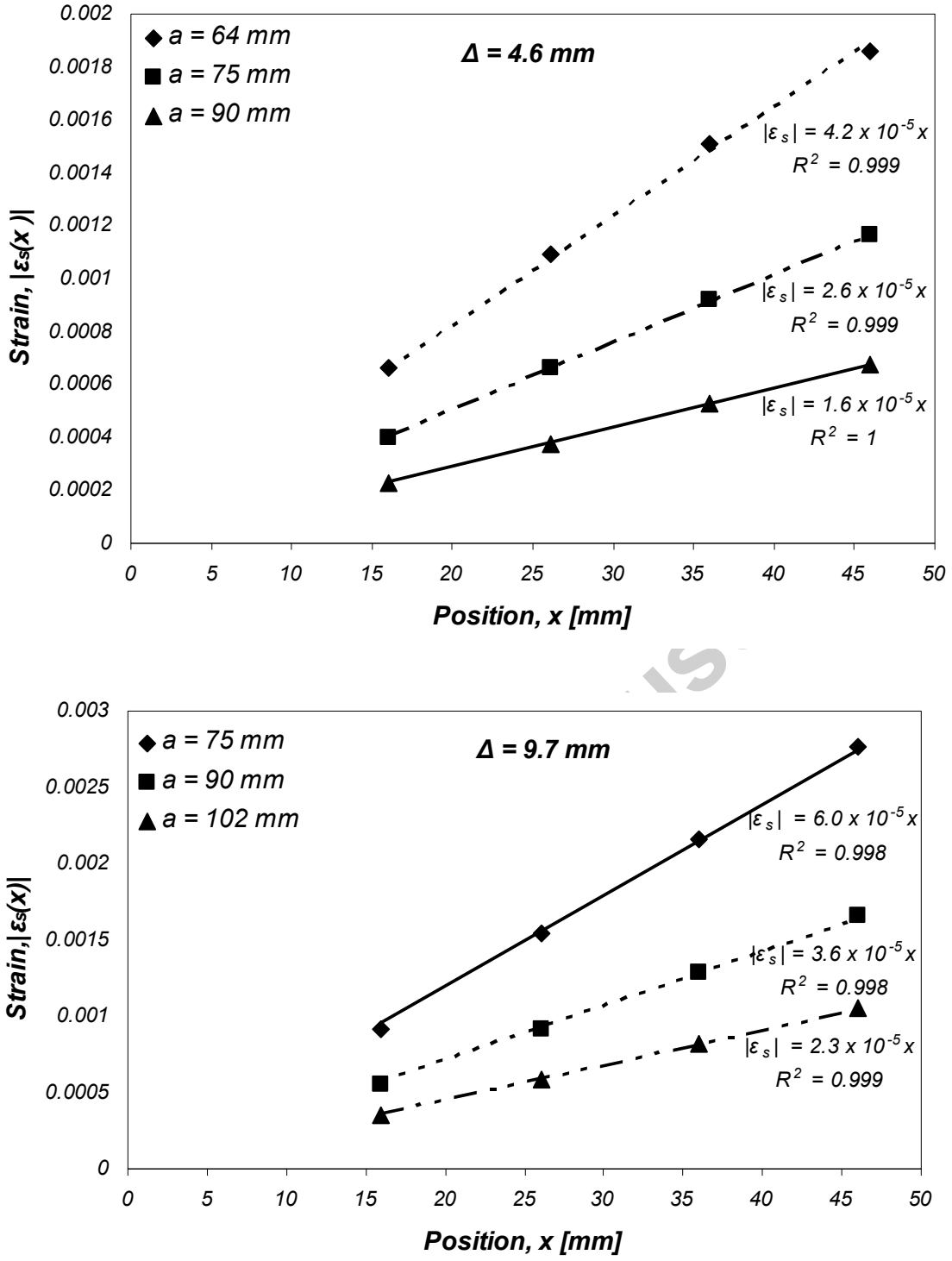


**Fig.4.** Surface strains, $|\varepsilon_s(x)|$, obtained from strain gauge measurements, *vs* positions, *x*, of strain gauges (*x* = 16, 26, 36 and 46 mm) and corresponding linear regression lines, for wedges of both thicknesses, 4.6 and 9.7 mm. The three lines in each graph correspond to imposed "crack lengths", *a*, given in the left upper corner.

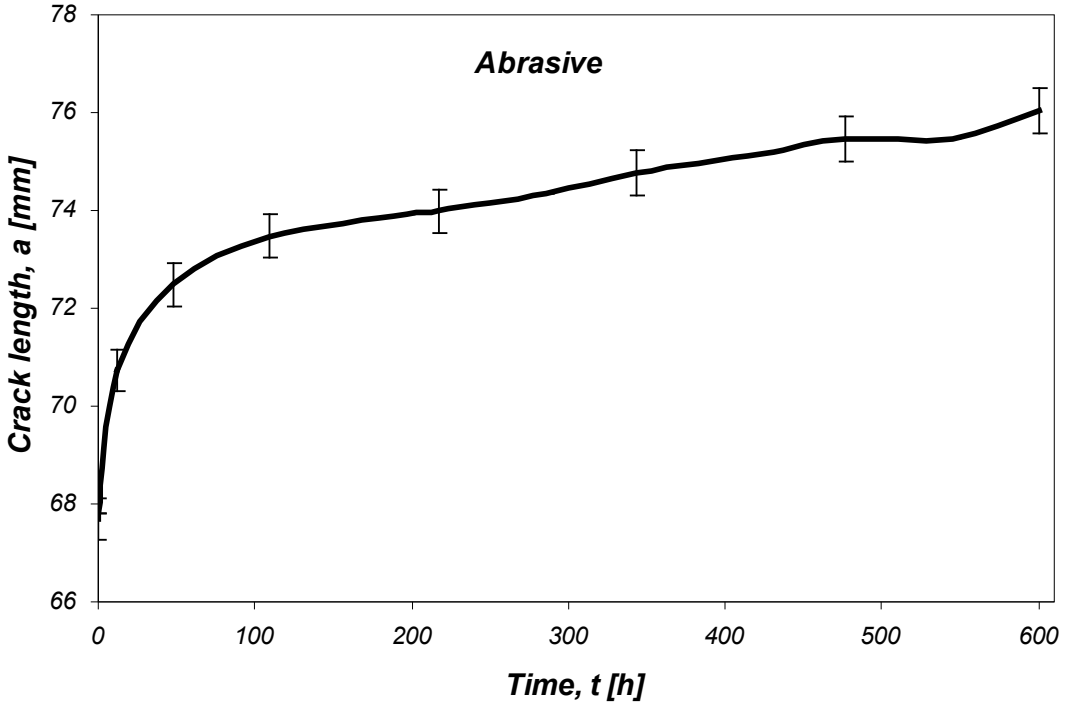


**Fig. 5.** Results of crack length, *a*, *vs* time, *t*, for wedge test with abrasive prepared surfaces.

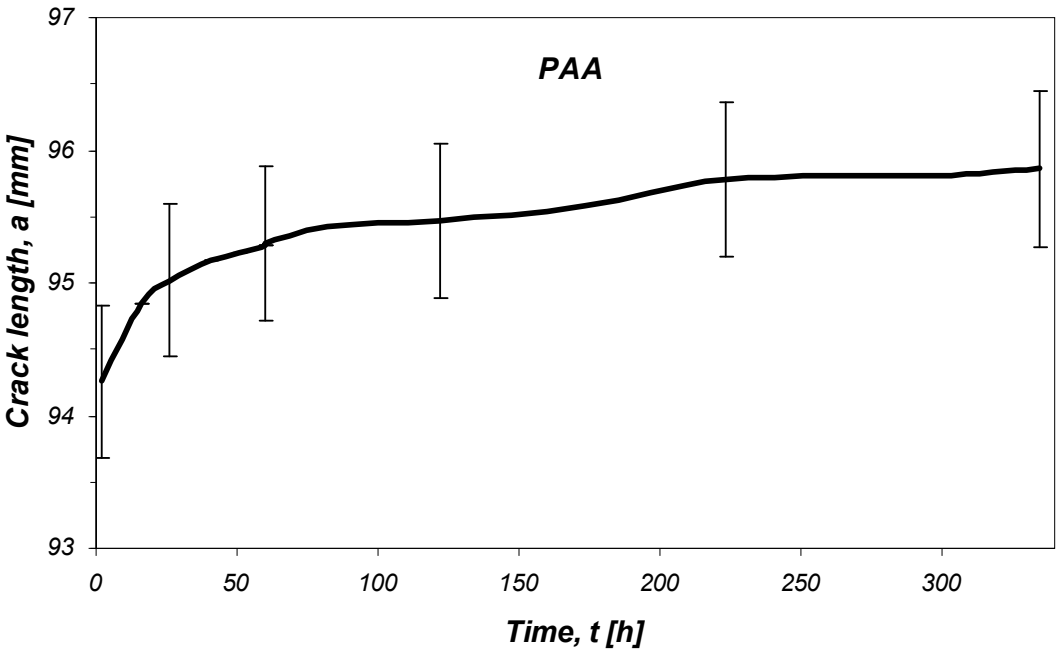


**Fig. 6.** Results of crack length, *a*, *vs* time, *t*, for wedge test with PAA prepared surfaces.

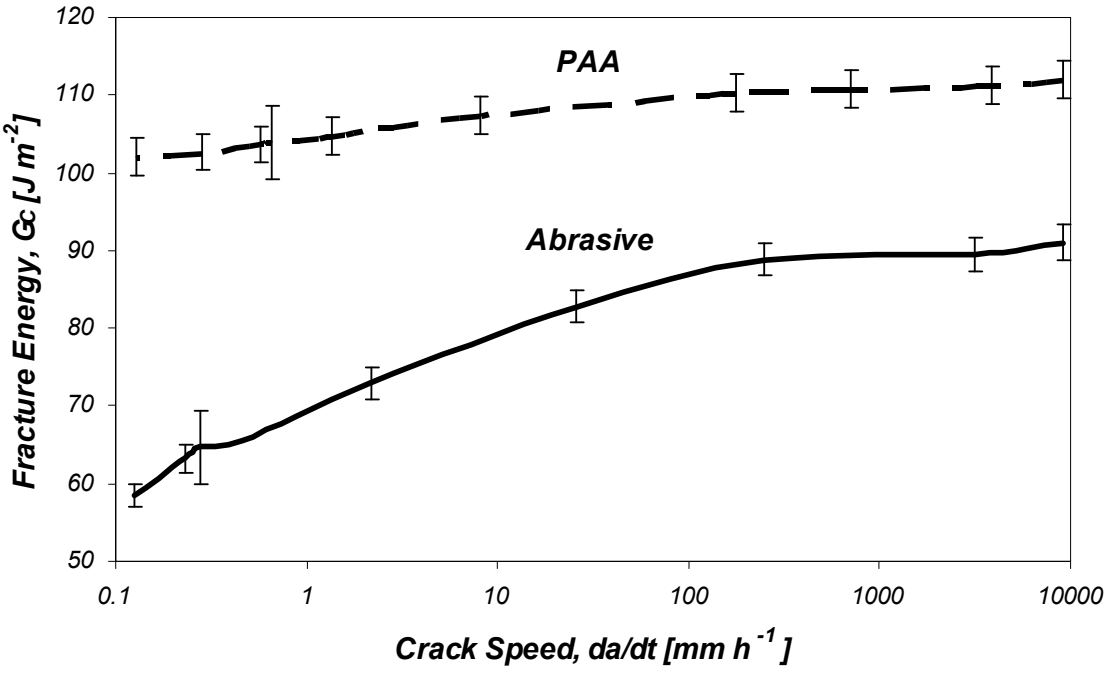


**Fig. 7.** Fracture, or adhesion, energy, $G_c$, *vs* crack growth rate, $da(t)/dt$, for wedge tests after abrasive and after PAA surface treatments prior to adhesive bonding with epoxy resin. Smaller error bars are only representative and could be calculated for any value of $da(t)/dt$. They correspond to the result of errors *only* on $a$. The two larger bars, one on each curve, represent overall errors taking into account systematic effects of $E$, $\Delta$ and $h$.

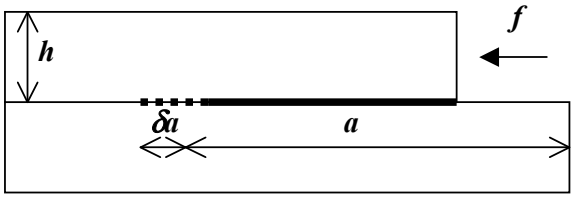


**Fig.A2.1** Model for mode II fracture.

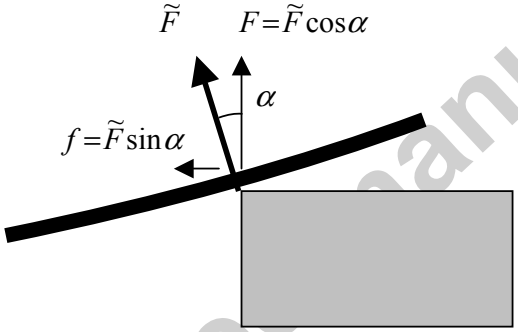


**Fig A2.2** Close-up of wedge/beam contact zone.